CHAPTER 5 EXPERIMENTAL PROCEDURE

The in-diffusion behaviour of silver together with the production, annealing of radiation damage and diffusion behaviour of implanted silver in single crystalline 6H-SiC have been investigated, using RBS, RBS-C and SEM, from temperatures below the melting point of silver (960 ^{o}C) up to 1600 ^{o}C. This chapter discusses all the experimental details of this investigation.

5.1 SAMPLE PREPARATION

The starting materials for this study were single crystalline 6H-SiC wafers from Intrinsic Semiconductor in Dallas VA/USA, with a diameter of 50.8 mm, thickness of 368±25 μm and micropipes area density < 30 cm^{-2}. Before deposition or implantation the wafers were cut into halves using a diamond scriber. For silver deposition experiments, the halves were further cut into 5×5 mm^2 samples with a rotary diamond saw before being cleaned in an ultrasonic bath using acetone (10 min), trichloroethylene (10 min), 10% hydrochloric (HCl) acid (10 min) and 10% dilute hydrofluoric (HF) acid (10 min) successively, with rinsing by de-ionised water after each step. Finally the water was blown away using nitrogen gas. The cleaning procedure was employed to remove any contamination together with the natural oxide layer on the surface, which might have had negative effects on the experiment. The size of the samples was chosen to suit the RBS-C and SEM analyses experiments. For the deposition of silver (100 nm), the cleaned samples were mounted on a steel holder (which holds eight samples), then transferred into a vacuum. This was done to ensure that they were prepared under the same conditions. The deposition of silver of 100 nm thickness is discussed in section 5.2. After deposition some of the samples were encapsulated in a quartz ampoule together with a silver source to maintain a silver layer on the samples' surfaces and then annealed. The silver source was included to maintain a silver layer on these surfaces during annealing.

The other halves of the samples were cleaned four times in an ultrasonic bath with acetone (10 min) followed by de-ionised water rinsing at the end of the four cleaning steps and then sent for implantation. This procedure was followed to remove

contamination on the surfaces that was introduced during the cutting process. The oxygen layer on the surface does not affect implantation so negatively because the implants are inside the samples. After implantation, discussed in section 5.3, the samples were also cut into 5×5 mm^2 samples and cleaned with acetone for RBS-C, SEM and annealing experiments. Figure 5-1 depicts the typical processes of sample preparation.

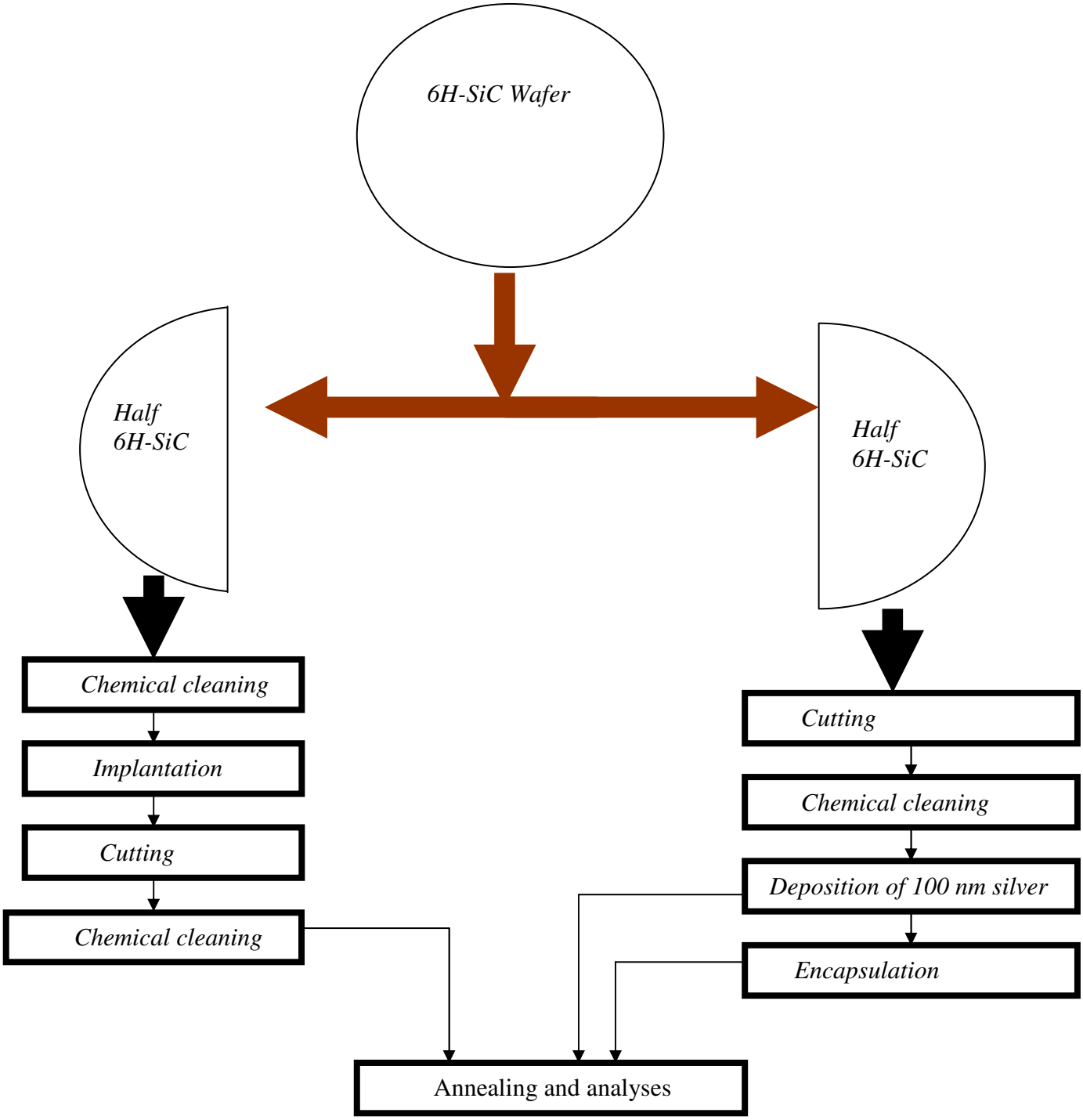

Figure 5-1: A diagram showing the typical process of sample preparation.

5.2 DEPOSITION

A thin silver film of 100 nm thickness was deposited on some 6H-SiC substrates mounted on the steel holder (capable of holding eight 5×5 mm^2 samples) using a resistive evaporation technique. This was performed under a vacuum of about 10^{-4} *Pa.* In this system, the substrates were placed in a high-vacuum chamber with a

molybdenum crucible containing the silver to be deposited, a shielding plate located between the crucible and substrates and a water cooled film thickness monitor (see figure 5-2).

For the deposition of silver, a current of about 4A was applied through the molybdenum crucible until it heated up beyond the boiling point of silver, thereby causing the latter to evaporate and condense on all the exposed cooled surfaces on the vacuum chamber. The deposition is only performed on the side facing the crucible as seen in figure 5-2, which illustrates the deposition process that is taking place in the vacuum chamber. After deposition some of the samples, together with a silver source, were vacuum-encapsulated to about 10^{-6} mbar with a quartz glass ampoule and then annealed. The silver source was included in the ampoule so that the silver vapour equilibrium was reached in a very short time, thus maintaining the silver layer on top of the samples.

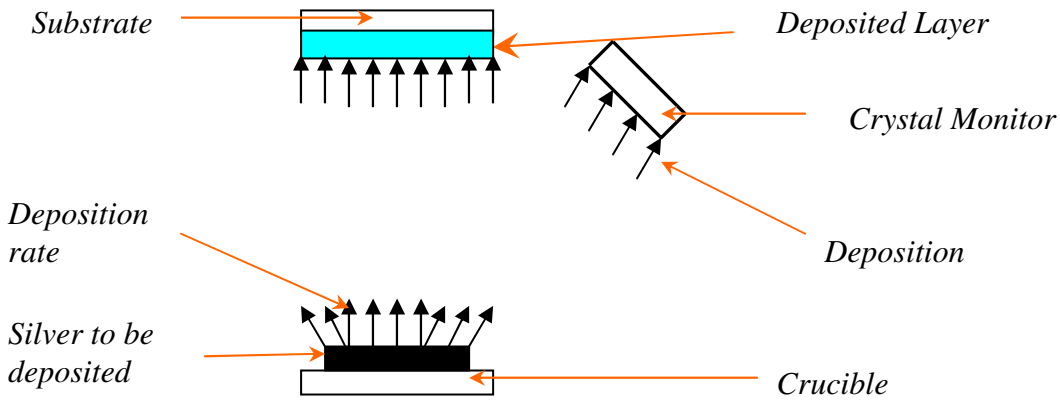

Figure 5-2: A schematic representation of the Ag deposition process in a vacuum chamber. The shielding plate is not shown.

5.3 IMPLANTATIONS

All the implantations for this thesis were performed in the Institut für Festkörperphysik, Friedrich-Schiller-Universität, Jena, Germany. The silver ions ($^{109}Ag^{+}$) were implanted at an energy of 360 keV with a fluence of 2×10^{16} cm^{-2} for all the samples.

For the study of radiation damage and its influence on silver diffusion, silver was implanted at different temperatures, i.e. room temperature, 350 ^{o}C and 600 ^{o}C. To avoid the channelling of silver ions during implantation in single crystalline silicon carbide (6H-SiC), samples were tilted 7^{o} with respect to the normal incidence. All the implantations were performed at an average vacuum of 10^{-4} Pa. The flux was always kept below 10^{13} cm^{-2}s^{-1} to prevent beam induced target heating.

5.4 ANNEALING SYSTEMS

Two annealing systems were used in this study. For the in-diffusion experiments, the samples were vacuum annealed in a tube oven with a maximum temperature of 1000 ^{o}C. This maximum temperature is reached in the centre of the oven and slightly decreases towards the sides of the oven. A thermocouple with feedback to the control system regulates the temperature of the oven with an accuracy of ±5 ^{o}C. For the in-diffusion studies two experiments discussed in section 5.1 and 5.2 were performed: vacuum-encapsulated samples and un-encapsulated samples annealed in vacuum. For annealing, the samples were placed on a quartz glass supporting rod centred on the axis of a quartz tube attached to a turbo pump vacuum system. The quartz tube was then evacuated to about 10^{-6} mbar. The temperature of the sample was measured with a thermocouple near the sample. Before annealing was performed, the oven was allowed to stabilize at the preset temperature before shifting it to a position where the sample was centred in the middle of the oven for annealing. At the end of the annealing time, the oven was shifted back and the sample was then allowed to cool down to room temperature before samples were taken out for analyses. All the in-diffusion studies were conducted in this oven.

Implanted samples were annealed in vacuum using a computer controlled Webb 77 graphite furnace either for 10 hours (annealing cycles up to 80 hours or 30 minute annealing cycles up to 120 minutes), from 700 ^{o}C, a temperature below the melting point (962 ^{o}C) of silver, to 1600 ^{o}C. Three types of experiments were performed in this study: isochronal, sequential and isothermal annealing. During isochronal annealing different samples were subjected to different annealing

temperatures for the same time or annealing cycle while during isothermal annealing the samples were annealed at the same temperature, and the annealing time was incremented after analyzing the sample as *10h-analyses+10h = 20 hours-analyses+ 20 hours = 40 hours-analyses.* A similar procedure was followed with respect to isothermal annealing for 30 minute cycles. For sequential annealing experiments, samples were first annealed at a lower temperature, followed by analyses, and then taken to the next higher temperature, followed by analyses. The difference between sequential annealing and isochronal annealing is that in the former the time is not the same as in isochronal annealing. This was repeated until the highest temperature was reached.

The temperature is controlled by an Eurotherm 2704 controller connected to a thermocouple and a pyrometer. The temperature is measured by the thermocouple below 1475 °C and by the pyrometer above 1525°C. An average value of the thermocouple and pyrometer values is used between these temperatures. The temperature accuracy is ±15°C.

The silver implanted samples were sandwiched between two poly-crystalline silicon carbide slabs (see figure 5-3) and placed in a graphite crucible before annealing. This process was carried out to avoid contamination of the samples with any contaminants in the oven during annealing and to minimize the thermal etching of SiC in the sample of interest during annealing. Then the graphite crucible was put inside the oven. The system was subsequently evacuated to a pressure in the 10^{-6} mbar range and then degassed at 100 ^{o}C for 3 hours, annealed at the required temperature and time, finally being cooled down to room temperature - see figure 5-4. The aim of the degassing procedure was to ensure that the maximum pressure during annealing was in the 10^{-5} mbar range and to reduce the pumping time to attain a pressure lower than 5×10^{-6} mbar before annealing.

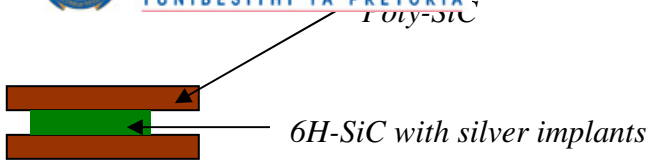

Figure 5-3: Diagram showing 6H-SiC with silver implants sandwiched between poly-silicon carbide.

A typical heating curve is depicted in figure 5-4 for a sample annealed at 1300 ^{o}C for 10 hours. Figure 5-4 portrays the time dependent relationships between (i), temperature and vacuum pressure (ii), vacuum pressure and heating current and (iii), cooling rates (^{o}C/min) and temperature during the degassing, heating up, annealing and cooling down processes. In figure 5-4, the repeated labels indicate the same process occurring.

If the heating element is switched on, a large current of 40A (G in figure 5-4(ii)) is used before the regulating process is started. After regulation, the current drops to 22A. The high heating rate (due to the large current) causes an initial high degassing rate of the heating element and nearby isolation material which results in an increase in the vacuum pressure from 10^{-6} mbar to about 10^{-5} mbar (J in figure 5-4). During this period the thermocouple in the oven is still at room temperature. During the heating up process, the pressure increases nearly linearly as a function of time to a maximum value of about 10^{-5} mbar at the start of the annealing dwell (E and C in the figure 5-4 (i)) while simultaneously the heating current increases (M in the figure 5-4(ii)) to about 40 A. This ensures a 20 °C/min heating rate. During the annealing dwell (C and D) the heating current stabilises at 22A while the pressure decreases to a minimum value of 10^{-6} mbar at the end of the dwell. This means that the pumping rate is larger than the degassing rate. The behaviour is identical during the degassing process - see A, B, J, E and F in figure 5-4(i). At the end of the annealing time, the heating current is switched off, causing a sharp drop in the vacuum pressure. The initial cooling rate is -19°C/min. In approximately 60 min the cooling rate increases to -4 °C/min (figure 5-4 (iii)). The duration of the heating ramp is 10 h and the heating rate is 20 °C/min; consequently the thermal stresses in the sample are greater during heating than during cooling. The system is allowed to cool down to a temperature below 100 °C and then flooded with argon gas, followed by vacuum pumping to increase the cooling rate until the temperature is below 40 °C

(where the samples are removed). Heat losses from the system occur by means of radiation and conduction in the isolation material and the container.

From the radiation law, the cooling of our oven is given by $T(t) = F\exp(-Zt)$.The cooling rate can be found by taking the derivative of the decrease in temperature with respect to time: $\frac{dT}{dt} = -FZ\exp(-Zt)$, where F and Z are constants and t is time. The values of F and Z were obtained by fitting the data of the cooling curve of temperature (^{o}C) versus time (h) as shown in figure 5-5 and were found to be 3.09×10^{6} ^{o}C and 2.79×10^{-1} h^{-1} respectively. The difference between the data and the fitted exponential curve is due to the fact that heat is not only lost via radiation and conduction as explained above. Figure 5-6 depicts the cooling curve for a sample annealed at 1300 ^{o}C for 10 hours compared to that for samples annealed at 1300 ^{o}C for 30 minutes. For a shorter annealing time, the cooling rate is very fast because the heat is not distributed to all parts of the oven, making cooling more rapid than that after a longer annealing time.

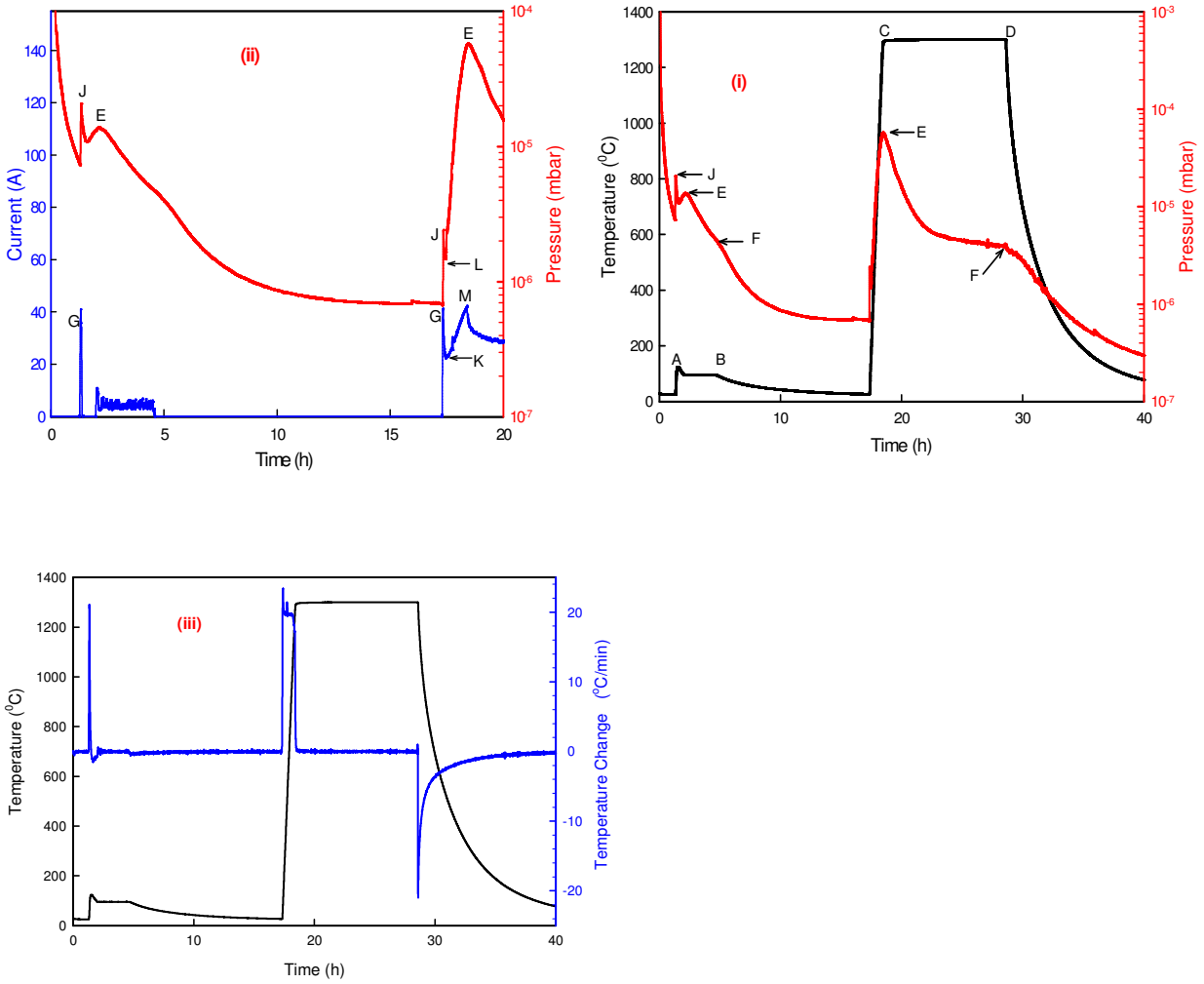

Figure 5-4: The typical heating curve as the function of time compared with pressure, current, heating and cooling rate during degassing (2h-10h), heating up (17h-30h), annealing (20h-30h) and cooling down (30h-40h).

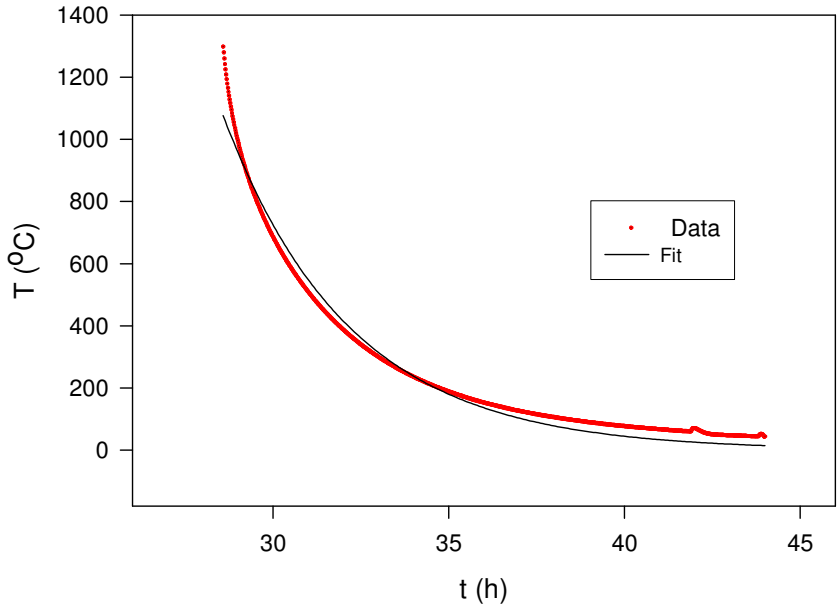

Figure 5-5: The cooling curve of the Webb oven as fitted to an exponential function to obtain constants.

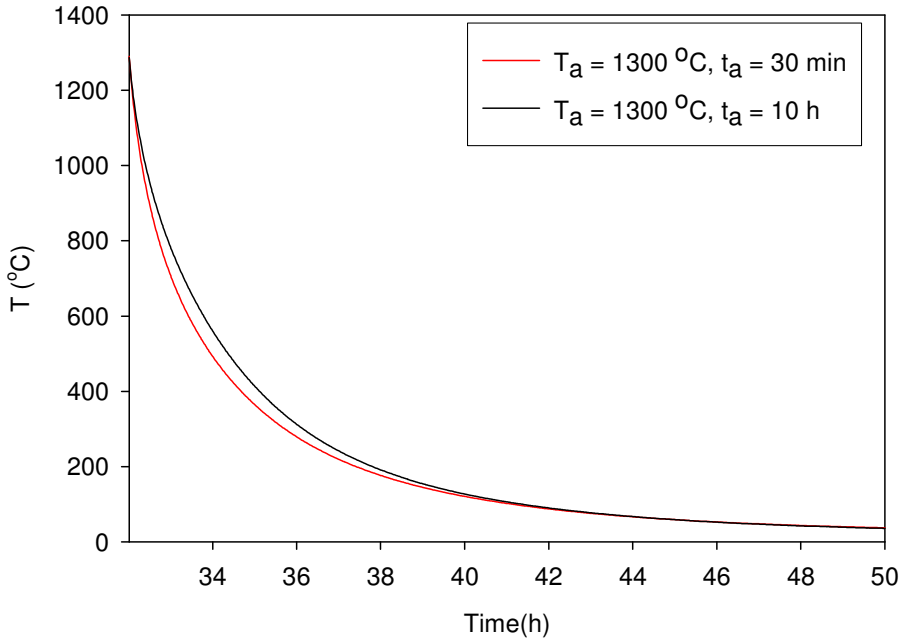

Figure 5-6: The cooling curve for a sample annealed at 1300 °C for 10 h compared to the cooling curve for a sample annealed at 1300 °C for 30 minutes.

5.5 DATA ACQUISITION

The block diagram of the apparatus used in the detection, amplification and collection of backscattered alpha particles is depicted in figure 5-7. These particles are detected by a Si-surface barrier detector. The signal produced was first amplified by the pre-amplifier Canberra 220 before being fed into the main amplifier, a Tennelec TC 243. This Si-surface barrier detector requires a biased voltage of 40 V.

The bipolar (bi) output signal from the amplifier is fed into the digital oscilloscope for beam monitoring purposes while the unipolar (Uni) signal is fed into the multi-channel analyzer (MCA). On the other hand, the current collected at the back of the target is fed into the current integrator, an Ortec 439, where it is digitized. The logic signal from the current integrator is sent into a charge counter where its output is fed to the MCA and the counter. The logic signal from this current orders the MCA when to start processing the unipolar signal from the amplifier and when to stop. It also instructs the counter when to start counting and when to stop doing so.

Inside the MCA there is a single channel analyser (SCA). This selects the energy window by adjusting the lower and the upper energy discriminators on the SCA. This is done to allow only the signals with the energies within the energy window to be further processed. The logic output from the SCA (inside MCA) is fed into charge counter and is used in RBS-C for channel direction searching, as explained in section 4.2. Finally the output of the MCA is fed into the computer where it is accessible while being collected. The MCA output consists of backscattered counts (or yield) vs. channel numbers. The channel numbers have a linear relationship with the backscattered energy of particles.

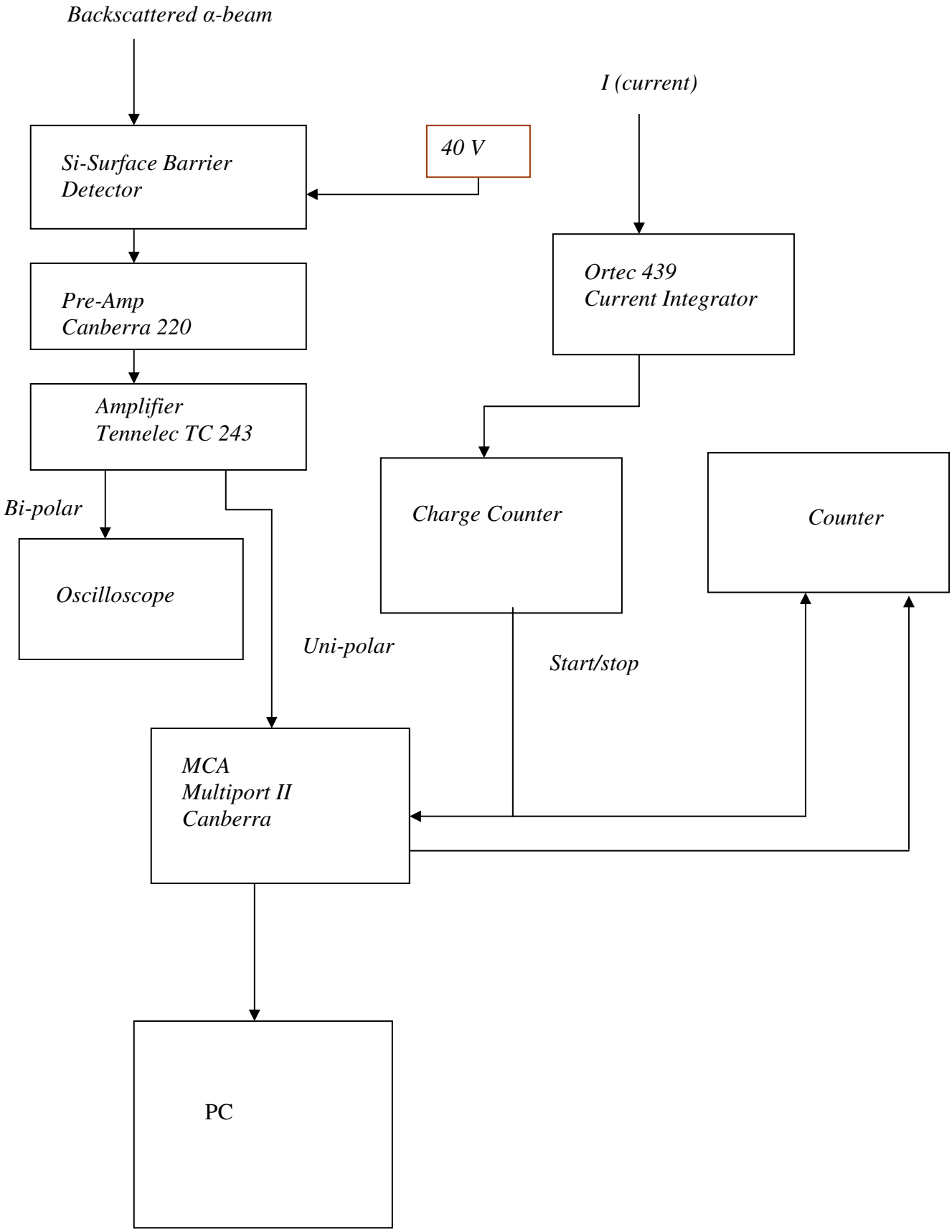

Figure 5-7: Block diagram of the electronic circuit for RBS and RBS-C measurements.

5.6 DATA ANALYSES

Counts versus channel number were obtained by collecting a total charge of 8 μC per run for 10 runs per sample under investigation: the average of the runs was used for further analyses of the data. This process was carried out in order to reduce the statistical error. All the spectra were stored in the computer connected to the MCA before they were taken for further analyses. The energy calibration required for depth profile analyses was calculated from the RBS spectrum of glassy carbon with a 10 nm layer of silver on top using 1.6 MeV α -particles.

The energy calibration in keV/channel was converted into a depth calibration nm/channel using a computer program, STOP2 [Fri06], which makes use of the energy loss data in Ziegler [Zie77]. Assuming no loss of silver, the counts were converted into relative atomic density (%) by first calculating the silver density inside SiC. This was achieved by taking into consideration the implanted fluence (ϕ) in cm^{-2} unit, the total silver counts (*N*) in *counts* unit, count per channel (*dn*) in *counts* unit and the depth resolution (*D*) in *cm/channel* unit:

$$\rho_{Ag} = \frac{\phi dn}{ND} (\text{Ag-atoms/cm}^3) \qquad \ldots 5.1$$

Thereafter the relative atomic density (*RAD*) % was determined by taking the ratio:

$$RAD(\%) = \frac{\rho_{Ag}}{\rho_{SiC}} \times 100 \qquad \ldots 5.2$$

Where ρ_{Sic} is the atomic density of SiC in cm^{-3}. For this study the density of 6H-SiC was taken to be 3.21 $g.cm^{-3}$, equivalent to 9.641×10^{22} $atoms/cm^3$.

The spectra of RAD % versus depth or of counts versus depth were then fitted to an Edgeworth distribution using the Genplot fitting function program [www2] to obtain the first four moments of the silver distribution function i.e. projected range/mean depth (Rp), straggling/standard deviation (σ), skewness (γ), and kurtosis (β). These

are mathematically written as follows:

$$R_p = \frac{\sum_i x_i}{N},\ \sigma = \left[\frac{\sum_i x_i - R_p}{N}\right]^{\frac{1}{2}},\ \gamma = \frac{\sum_i (x_i - R_p)^3}{N\sigma^3} \text{ and } \beta = \frac{\sum_i (x_i - R_p)^4}{N\sigma^4}$$

where x_i is the distance from the surface to the implanted ions and N is the number of implanted ions. For a normal distribution or Gaussian distribution $\gamma = 0$ and $\beta = 3$. The Edgeworth distribution is shown below:

$$f(x) = g(x)p(x) \qquad \ldots.5.3$$

Where

$$g(x) = \frac{h}{\sqrt{2\pi}}\exp(\frac{-\arg(x)}{2})$$

and

$$p(x) = 1 + \frac{\gamma \arg(x)^3 - 3\arg(x)}{6} + \frac{(\beta - 3)(\arg(x)^4 - 6\arg(x)^2 + 3)}{24},$$

with

$$\arg(x) = \frac{(x - R_p)}{\sigma}$$

and where h is the height fitting parameter.

Skewness characterizes the degree of asymmetry of a distribution. Positive skewness indicates a distribution with an asymmetric tail extending towards more positive values, while negative skewness indicates a distribution with an asymmetric tail extending towards more negative values. Our profiles show a positive skewness, indicating that our distributions are skewed towards the more positive value. Kurtosis measures how peaked or flat the distribution is with respect to the Gaussian function. The full width at half the maximum of the silver peak is given by: $FWHM = 2\sigma\sqrt{2\ln 2}$.

For our diffusion analyses the FWHMs of the depth profiles of the annealed samples were compared with the FWHMs of the as-implanted profiles. The depth profiles of SiC were calculated using the Si depth resolution from STOP2. The relative disorder was estimated by taking the ratio of the aligned/channelled spectrum to the random spectrum. The retained silver was calculated by working out the ratio of total silver

(as-implanted silver) to the total silver left behind (normalized to the as-implanted RBS spectrum).

5.7 ERROR ANALYSES

The errors for measurements given in this study were calculated from several uncertainties: statistical uncertainty σ_s, which was minimized by collecting a charge of 8 μC, the uncertainty from genplot, σ_g, 1% uncertainty of the analyzing beam energy, σ_b and 1% uncertainty of the scattering angle, σ_a. The total error was then calculated by summing the squares of the functions of these errors and taking the square root: $\sigma_t = \sqrt{f^2(\sigma_s) + f^2(\sigma_s) + f^2(\sigma_g) + f^2(\sigma^2)}$.

5.8 REFERENCES

[Zie77] J.F. Ziegler, The Stopping and Ranges of Ions in Matter, Pergamon Press, New York (1977).

[Fri06] E. Friedland, STOP2, Private communication, Department of Physics, University of Pretoria, 2006.

[www2] hhttp://www.genplot.com, 4 November 2009.

[www1] http://www.canbera.com/products/genie2000, 4 November 2009.